Pflugers Arch - Eur J Physiol (2014) 466:491–504
DOI 10.1007/s00424-013-1332-y

ION CHANNELS, RECEPTORS AND TRANSPORTERS

Isoform- and receptor-specific channel property of canonical transient receptor potential (TRPC)1/4 channels

Jinsung Kim · Misun Kwak · Jae-Pyo Jeon · Jongyun Myeong · Jinhong Wie · Chansik Hong · Sung-Young Kim · Ju-Hong Jeon · Hyun Jin Kim · Insuk So

Received: 6 March 2013 / Revised: 29 July 2013 / Accepted: 29 July 2013 / Published online: 16 August 2013

Abstract Transient receptor potential canonical (TRPC) 1, the first mammalian homologue of *Drosophila trp* gene, is distributed widely in mammalian cells and is involved in many physiological functions. TRPC1 is reported to be functional following heteromeric formation with other TRPC channels such as TRPC4 or TRPC5. It is known that the composition of this widely distributed TRPC1 is far from simple; functionality of such channels has been highly controversial. Furthermore, TRPC1 gene is known to have two splicing variants; one encodes long (TRPC1α) and the other encodes short (TRPC1β) TRPC1 isoforms, respectively. In this study, we examined the functionality of TRPC1/4 channels using various activation systems. $G_{q/11}$-coupled receptor (e.g., M1 or M3 receptors) stimulation significantly increased TRPC1α/4 currents but induced mild activation of TRPC1β/4. In addition, when expressed with TRPC4, TRPC1α acted as a pore-constituting subunit and not a β ancillary subunit. Multimerized with TRPC4, TRPC1α also generated strong pore field strength. We also found that $G_{i/o}$-coupled receptor (e.g., M2 receptor) stimulation was insufficient to activate TRPC1α/4 and TRPC1β/4 channels but selectively activated TRPC4 homomeric channels. These findings demonstrate that TRPC1/4 channel shows dynamic gating property depending on TRPC1 isoform subtypes and receptor stimulation system. Therefore, careful discrimination of the specificity of TRPC1 isoforms and upstream activation system is important in thorough understanding of TRPC1 and TRPC1/4 channels.

Keywords TRPC1 · TRPC4 · G-protein coupled receptor (GPCR) · M1 · M2 · M3 · Splicing variant · Muscarinic stimulation · Inhibitory G-protein (G_i) · Receptor-operated Ca^{2+} entry (ROCE)

Abbreviations

TRPC	Transient receptor potential canonical
TRPC1α	human TRPC1 isoform long
TRPC1β	human TRPC1 isoform short
CCh	(2-Hydroxyethyl)trimethylammonium chloride carbamate

Jinsung Kim and Misun Kwak contributed equally to this work and should be considered as co-first authors.

Electronic supplementary material The online version of this article (doi:10.1007/s00424-013-1332-y) contains supplementary material, which is available to authorized users.

J. Kim
Department of Chemistry, Korea Advanced Institute of Science and Technology, Daejeon 305-701, Republic of Korea

J. Kim · M. Kwak · J.-P. Jeon · J. Myeong · J. Wie · C. Hong · S.-Y. Kim · J.-H. Jeon · I. So (✉)
Department of Physiology, Seoul National University College of Medicine, Seoul 110-799, Republic of Korea
e-mail: insuk@plaza.snu.ac.kr

H. J. Kim (✉)
Department of Physiology, Sungkyunkwan University School of Medicine, Suwon 440-746, Republic of Korea
e-mail: kimhyunjin@skku.edu

Introduction

Transient receptor potential gene (*trp*) was first discovered in *Drosophila melanogaster*. *trp*$^{-/-}$ flies showed transient but not sustained membrane depolarization after exposure to light in electroretinogram [19, 39]. The first mammalian homologue of d*trp* (*Drosophila trp*) gene was successfully cloned by two groups independently in 1995, named Htrp-1 and hTRPC1, respectively [41, 44]. Subsequently, the first mammalian homologue, transient receptor potential canonical 1 (TRPC1), has been the focus for intensive research and its organ/tissuespecific distribution and the functional characteristics were widely acknowledged in over a decade [2, 27]. Among TRPC1, TRPC4, and TRPC5 channels, which share high amino acid similarity (~40 %), TRPC1 has been shown to be distributed ubiquitously (such as in the brain, heart, ovaries, testis, liver, kidney, vascular smooth muscle, gastrointestinal (GI) tract, salivary glands, endothelium, etc.) [2]. More importantly, TRPC1 is generally considered to be involved in many physiological functions, such as regulation of smooth muscle, endothelin-evoked arterial contraction, salivary gland secretion, endothelial permeability, glutamatergic neurotransmission, growth cone turning, etc. [2].

The widespread expression of TRPC1 in vivo suggests its multifaceted properties. Accordingly, in vivo and in vitro approaches show that the functionality of the channel is complicated. Some studies suggest that TRPC1 is one of the molecular candidates for store-operated Ca^{2+} entry (SOCE) that is distinguishable from Ca^{2+}-release activated channel (CRAC) current; TRPC1 showed lower Ca^{2+} selectivity than CRAC channels [1, 2, 18, 24]. Others report that heteromeric channel comprised of TRPC1 and TRPC5 (TRPC1/5) are gated by muscarinic receptor stimulation [33–35] and the channel opening is irrelevant to store-depletion status [34]. Extensive reviews covering the functionality of TRPC1 channels in details are published elsewhere [2, 20, 27, 40].

It is known that the two TRPC1 genes cloned in 1995 was not identical. One of them encodes human long TRPC1 gene [44] whereas the other is the alternative splicing short gene [41]. Although accumulating results clarify the functional property of TRPC1, discrimination between the two splicing variants is sparse. Undoubtedly, it is important to discriminate the specificity of TRPC1 isoforms and their functionalities, e.g., TRPC4 isoforms have distinct characteristics in view of PIP_2 binding affinities [23], concurrently different gating property. Similar differences have been described in details for transient receptor potential melastatin 3 channels [9, 22].

In a number of studies, we have shown that TRPC4 and TRPC5 channels are gated by muscarinic stimulation and thereby these channels are classified as receptor-operated channels. Although receptor-operated TRPC4 may have been confined by classical $G_{q/11}$-PLC pathway, recently we have also shown that $G_{i/o}$-coupled receptor stimulates (e.g., M2 stimulation) TRPC channels [15].

In this paper, we validated functional characteristics of TRPC1 and TRPC1/4 channels based on the questions raised above. We prepared both unspliced TRPC1 and alternatively spliced TRPC1 and examined their electrophysiological characteristics. We examined whether TRPC1 contributes to form a distinct ion channel pore following heteromeric formation with TRPC4. We also investigated if $G_{i/o}$-coupled receptor stimulation is sufficient to activate TRPC1/4 heteromeric channels.

Materials and methods

Cell culture and transient transfection

Human embryonic kidney (HEK293) cells (ATCC, Manassas, VA) were maintained according to the supplier's recommendations. For the transient transfection, the cells were seeded in 12-well plates. The following day, 0.5~1 g/well of cDNA was transfected using the transfection reagent FuGENE 6 (Roche Molecular Biochemicals), as detailed in the manufacturer's protocol. Co-expression of TRPC channels with the receptor stimulation system was achieved using a TRPC1 channels to TRPC4 channels to receptor transfection ratio of 2:2:1. Empty vectors (e.g., pcDNA3.1, ECFP-C1, EYFP-C1) were used for corresponding control expressions. After 30–40 h, the cells were trypsinized and transferred to a small recording chamber for whole-cell recording.

Cloning and mutagenesis

Human TRPC1 isoform long cDNA (GenBank ID: U31110, UniProt ID: P48995-1) inserted in pcDNA3.1 vector or pIRES2-EGFP vector was kindly donated by Dr. Michael Mederos. Human TRPC1 isoform short cDNA (GenBank ID: U31110, UniProt ID: P48995-2) was cloned in our hands by performing deletion mutation using sense primer 5′-CTTTTGGACTACGGTTGTCAGAAACTAATGGAACGAATTCAG-3′ and anti-sense primer 5′-CTGAATTCGTTCCATTAGTTTCTGACAACCGTAGTCCAAAAG-3′. Pore-dead mutation switching three amino acids L, F, and W at position 594, 595, and 596 to alanine of human TRPC1 isoform long was achieved by using sense primer 5′-GCCACCTGCTTCGCTGCGGCCGCGTATATTTTCTCCTTAGCG-3′ and anti-sense primer 5′-CGC TAAGGAGAAAATATACGCGGCCGCAGCGAAGCAGGTGGC-3′. All mutagenesis was conducted using QuikChange site-directed mutagenesis kit (Stratagene). cDNA of human TRPC1 isoform long tagged with CFP at N-terminus was kindly donated by Dr. Vaca Luis. Mouse TRPC4 isoform short cDNA (GenBank ID: U50921.1, UniProt ID: Q9QUQ5-2) was kindly donated by Dr. Michael Schaefer. DNA sequences encoding the channel was truncated by BglIII and SalI restriction enzymes and inserted into pEGFP-N1 vector. Mouse TRPC5 cDNA (GenBank ID: AF029983, UniProt ID: Q9QX29) inserted in pIRES2-EGFP vector was kindly donated by Dr. Michael Mederos.

Human muscarinic acetylcholine receptor types 1, 2, 3, and alpha subunit of intrinsic GTPase-deficient mutant (constitutively active form) of inhibitory heterotrimeric G-protein type 2 ($G\alpha_{i2}$) in pcDNA3.1+ vector were all purchased from Missouri S&T cDNA resource center (Missouri, USA). Rat histamine receptor type 1 in pEGFP-N1 vector was kindly donated by Dr. Young Duk Yang.

Electrophysiology

The cells were transferred to a small chamber on the stage of an inverted microscope (Eclipse Ti, Nikon, Japan) and attached to coverslips in the small chamber for 10 min prior to the patch recording. Glass microelectrodes with 2–2.5 MΩ resistance were used to obtain gigaohm seals. The bath solutions were constantly perfused with an extracellular solution at a rate of 1–2 ml/min. The currents were recorded using an Axopatch 200B patch-clamp amplifier (Axon Instruments, USA). The current was recorded for 550-ms duration ramps from +100 to −120 mV with time resolution of 0.4 mV/ms and with a holding membrane potential of −60 mV. pCLAMP software v.10.2 and a Digidata 1440A (Axon Instruments) were used for data acquisition and application of the command pulses. The data were filtered at 5 kHz and displayed on a computer monitor. The data were analyzed using pCLAMP v.10.2 and Origin Pro 8 software (OriginLab, MA, USA). For recordings of the TRPC channels, we used normal Tyrode solution unless otherwise mentioned and occasionally Cs^+-rich external solution. The normal Tyrode solution contained 135 mM NaCl, 5 mM KCl, 2 mM $CaCl_2$, 1 mM $MgCl_2$, 10 mM glucose, and 10 mM HEPES with a pH of 7.4 adjusted with NaOH. The Cs^+-rich external solution contained equimolar CsCl rather than NaCl and KCl. pH was adjusted to 7.4 using CsOH. For receptor stimulation, 100 μM carbachol (carbamoylcholine chloride) and 10 μM histamine (histamine dihydrochloride) was added to each extracellular bath solution. The internal solution contained 140 mM CsCl, 10 mM HEPES, 0.2 mM Tris–GTP (Tris-guanosine 5′-triphospate), 0.5 mM EGTA, and 3 mM Mg-ATP (adenosine 5′-triphosphate) with a pH of 7.3 adjusted with CsOH.

For analysis of cationic conductance activation curves, each group of conductance–voltage (G, V) data points were fitted by Boltzmann equation in the following form:

$$G = \frac{-G_{max}}{1 + exp\left[\left(V - V_{1/2}\right)/k\right]} + G_{max}$$

where G is cationic conductance (siemens), $G_{\max}$ is the maximum conductance, $V_{1/2}$ is the potential at which G=0.5$G_{\max}$, and k is the slope factor (volts).

For analysis of relative monovalent cation permeability, the Goldman–Hodgkin–Katz equation [10, 12] in the following form was used:

$$\frac{P_X}{P_{Na}} = \frac{[X^+]_o}{[Na^+]_o} \times e^{\frac{\Delta E_{rev} F}{RT}}$$

where F is a Faraday constant, R is the gas constant, ΔE_{rev} is the difference in reversal potential (volts), and T is the absolute temperature (room temperature, 298.15 K). E_{rev} was corrected for liquid junction potential, which was achieved by using JPCalcW (Axon Instruments). For calculating molar concentrations of monovalent ions ($[X^+]_o$), activity coefficient (γ) of 0.75 was used for Na^+, Li^+, and Cs^+ ions. The Na^+-, Li^+-, and Cs^+-rich solution contained 2 mM $CaCl_2$, 1 mM $MgCl_2$, 10 mM glucose, 10 mM HEPES, and 140 mM NaCl, LiCl, and CsCl, respectively. pH was adjusted to 7.4 using NMDG-OH. All reagents were purchased from Sigma (Sigma Aldrich, USA)

FRET microscopy

Three Föster Resonance Energy Transfer (FRET) images (cube settings for CFP, YFP, and Raw FRET) were gained from a pE-1 Main Unit to three FRET cubes (excitation, dichroic mirror, filter) through a fixed collimator: CFP (ET435/20 m, ET CFP/YFP/mCherry beamsplitter, ET470/24 m, Chroma), YFP (ET500/20 m, ET CFP/YFP/mCherry beamsplitter, ET535/30 m, Chroma), and Raw FRET (ET435/20 m, ET CFP/YFP/mCherry beamsplitter, ET535/30 m, Chroma). The excitation LED and filter were sequentially rotated, and rotation period for each of filter cubes was ~0.5 s. All images (three for CFP/YFP/Raw FRET, respectively) were obtained within 1.5 s. Each image was captured on a cooled 10 MHz (14 bit) CCD camera (DR-328G-C01-SIL: Clara, ANDOR technology, USA) with an exposure time of 150 ms with 2×2 binning (645×519 pixels) under the control of MetaMorph 7.6 software (Molecular Devices, Japan). To obtain the FRET efficiency of a cell, we utilized a microscope (IX70, Olympus, Japan) with a ×60 oil objective and the three-cube FRET method calculation [8].

Surface Biotinylation

Cells were washed in PBS, and after washing in PBS, cells were incubated in 0.5 mg/ml sulfo-NHS-LC-biotin (Pierce) in PBS for 30 min on ice. Free biotin was quenched by the addition of 100 mM glycine in PBS. Lysates were prepared in lysis buffer by passing 7–10 times through a 26-gauge needle after sonication. Lysates were centrifuged at 13,300×g for 10 min at 4 °C, and protein concentration in the supernatants was determined. Forty microliters of a 50 % slurry of avidin beads (Pierce) was added to cell lysates (400 μg protein). After incubation for 1 h at RT, beads were washed three times with 0.5 % Triton X-100 in PBS, and proteins were extracted in sample buffer. Collected proteins were then analyzed by Western blot.

Sequence alignment

cDNA sequences and amino acids sequences, either aimed for material preparation or data analysis, were conducted by MultAlin webpage (http://multalin.toulouse.inra.fr/multalin/) [4].

Statistics

Results are expressed as means ±SEM. Results were compared using Student's t test between two groups or using ANOVA followed by post hoc test among three groups or more. $P<0.05$ was considered statistically significant. All statistical analysis was done with Origin Pro 8 software (OriginLab, MA, USA).

Results

TRPC1α homomeric channel is not affected by M receptor stimulation but contributes to a distinct pore formation with TRPC4

TRPC1α cDNA (human TRPC1 long gene) was expressed heterologously into HEK293 cells and co-expressed with human muscarinic receptor 1 (M_1R) and 3 (M_3R), respectively, to investigate the functional regulation of TRPC1α by muscarinic receptor stimulation. As shown in Fig. 1c, d, carbachol (CCh, 100 μM) stimulation of M_1R and M_3R did not affect TRPC1α (Fig. 1c, d). Similarly, the amplitude or the I–V relationship was not different from the currents measured from M_1R- and M_3R-only expressing cells (Fig. 1a, b).

Although homomeric TRPC1 is not regulated by CCh, it is possible that TRPC1 form an ion channel pore following heteromeric formation with TRPC4 channels. However, despite many reports regarding TRPC1, it remains elusive whether TRPC1 is the actual pore-constituting or not [13, 27, 29, 33–36]. Therefore, we hypothesized that TRPC1 may work as an ancillary subunit or another channel regulator aside from channel quartet.

We tested this hypothesis by expressing mouse TRPC4β with TRPC1α in M_1R or M_3R expressing cells. Co-expressed with TRPC4, TRPC1α was successfully translocated into plasma membrane which was not the case for single expression (Supplementary Fig. 1a). In other words, surface level of TRPC1α was dramatically increased when TRPC4 was co-expressed. Under these conditions, CCh elicited outwardly rectifying TRPC1α/4 currents (Fig. 1e, f). Similar results were also shown with TRPC1α/5 (Supplementary Fig. 2a, b). The TRPC1α/4 current is far different from that of TRPC4 since homomeric TRPC4 channels show double-rectifying I–V curves (Fig. 1g, h). The current densities of TRPC1α/4 currents at +80 and −60 mV were 30.9±14.8 and −2.8±1.5 pA/pF (M_1R stimulation) and 64.0±9.6 and −10.2±1.9 pA/pF (M_3R stimulation). TRPC4 currents at the same voltage points were 15.19±1.5 and −12.4±4.2 pA/pF (M_1R stimulation) and 26.0±11.3 and −24.9±13.7 pA/pF (M_3R stimulation) (Fig. 1i, left panel). Current ratio at +80 mV ($I_{+80\ \mathrm{mV}}$) and −60 mV ($I_{-60\ \mathrm{mV}}$) was devised as a rectification factor to show the sheer difference in I–V curve signature (Fig. 1i, right panel).

Moreover, another rectification factor parameterizing slope conductance at voltage regions from −120 to −80 mV ($g_{-120\sim-80\ \mathrm{mV}}$) and from 10 to 50 mV ($g_{10\sim50\ \mathrm{mV}}$) was designed to quantify the order of outward rectification. The idea was from analyzing conductance (G)–voltage (V) plot of two different I–V curves (Supplementary Fig. 3a, b). Owing to I–V signatures, G–V plot of TRPC1α/4 showed monotonic increase but TRPC4 showed typical N shape inflection. Curve fitting to Boltzmann equation resulted $V_{1/2}$ of −79.4±0.8 mV (TRPC4) and 29.5±1.7 mV (TRPC1α/4) with $G_{\max}$ of 25.0±0.3 nS (TRPC4) and 28.0±0.4 nS (TRPC1α/4) (Supplementary Fig. 3c). When we set two voltage intervals in G–V plot as mentioned above, we could observe clear conductance differences between two channels. This new rectification factor named after ρ (Rho) was 22.2±3.9 and 1.5±0.6 for M_1R-activated TRPC1α/4 and TRPC4 channels, respectively. M_3R-activated channels yielded 18.4±3.0 (TRPC1α/4) and 0.3±0.1 (TRPC4), respectively (Fig. 1j).

To determine whether TRPC1α contributes to form a distinct pore in TRPC1α/4 heterotetramer, we performed site-directed mutagenesis and cloned pore-dead mutant of TRPC1α, TRPC1$\alpha^{\mathrm{LFW/AAA}}$, based on putative pore-constituting amino acids [27]. The mutant TRPC1α (L, F, and W at position 594, 595, and 596 were switched to alanine) was expressed and we tested whether TRPC1$\alpha^{\mathrm{LFW/AAA}}$/4 heterotetramer remains functional in whole-cell recordings. As expected, cells expressing TRPC1$\alpha^{\mathrm{LFW/AAA}}$/4 lost the outwardly rectifying currents and showed only the double-rectifying ones. In addition, TRPC1$\alpha^{\mathrm{LFW/AAA}}$ yielded double-rectifying I–V curves when expressed with TRPC5 channels (Supplementary Fig. 2c, d). Moreover, current densities were decreased as the level of TRPC1$\alpha^{\mathrm{LFW/AAA}}$ expression with cDNA increased, without changing the I–V signature (Fig. 2a–c, left and right panel). These results suggest that mutation of the pore of TRPC1α/4 channels suppresses whole-cell current, yielding residual TRPC4 currents.

Although mutagenesis experiments suggest that TRPC1α may possess pore-constituting nature in its heteromeric formation, it is not known whether TRPC1$\alpha^{\mathrm{LFW/AAA}}$ co-assembles with TRPC4 and deprives its channel activity by collapsing the pore or it is merely an artifact from mutation. In order to isolate the variable, we co-expressed CFP-tagged TRPC1 with YFP-tagged TRPC4 and measured FRET efficiency. Both CFP-TRPC1α^{WT} and CFP-TRPC1$\alpha^{\mathrm{LFW/AAA}}$ showed significant FRET efficiency with YFP-TRPC4 (14.9±1.1 and 17.1±0.7 %) but not with YFP alone (1.6±0.8 and 3.4±1.3 %, Fig. 2d).

Taken together, these results suggest that TRPC1α alone does not form an ion channel in plasma membrane and thus not functional in response to muscarinic stimulation. However, it contributes to form a distinct pore in heteromeric formation with TRPC4. More specifically, TRPC1α is not a β

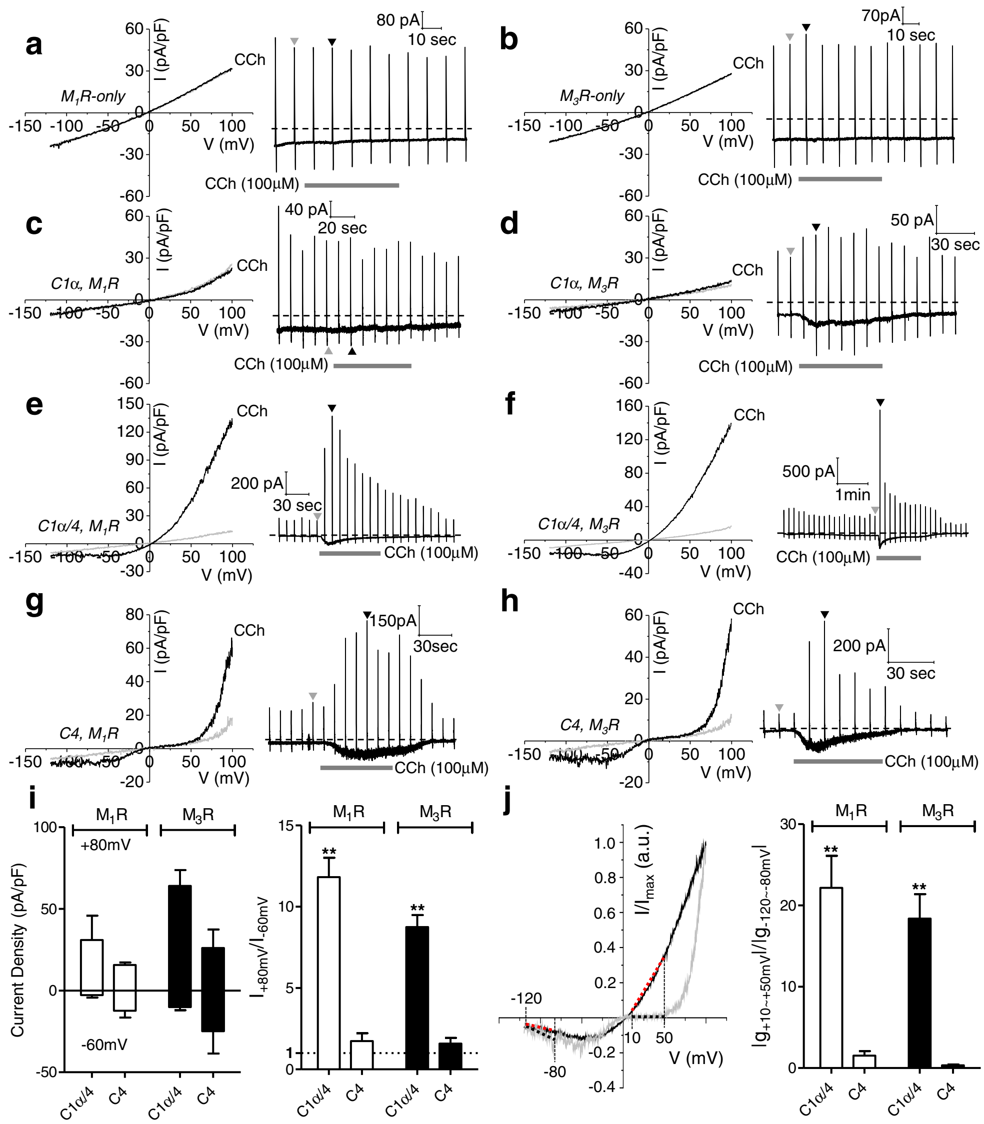

Fig. 1 $G_{q/11}$-coupled receptor stimulation and TRPC1α, TRPC1α/4, TRPC4 channel activity. From **a** to **h**, all *left panels* indicate *I–V* relationship and *right panels* indicate corresponding current traces. *Inset legends at upper left area of I–V curves* demonstrate heterologously expressed proteins. **a**, **b**In cells expressing M1 or M3 receptor, receptor stimulation by extracellular carbachol (100 μM) did not induced significant whole-cell current. **c**, **d**Cells expressing TRPC1α channels showed indistinguishable current increment in response to M1 or M3 stimulation achieved by extracellular carbachol (*CCh*, 100 μM). **e**, **f** Heteromeric TRPC1α/4 channel showed typical outward-rectifying *I–V* curves in response to M1 or M3 stimulation. **g**, **h** Genuine TRPC4 homomeric currents (without co-expression of TRPC1α) in response to M1 or M3 receptor stimulation. **i** *Left panel* indicates summarized current density measured above and *right panel* indicates rectification factor ($|I_{+80\ mV}/I_{-60\ mV}|$) analysis which was devised in order to show the sheer difference in *I–V* curve signature. **j** *Left panel* compares double-rectifying *I–V* curves of CCh-activated TRPC4 (*light gray*) and outward-rectifying *I–V* curves of CCh-activated TRPC1α/4 (*black*). In order to quantify the order of outward rectification, another rectification factor ρ (Rho) was devised which parameterizes two different slope conductance: $\rho \equiv |g_{+10\sim+50\ mV}|/|g_{-120\sim-80\ mV}|$. Two different *I–V* curves show stark difference in ρ value

ancillary subunit but α subunit that is readily assembled with other tetrameric constituents in equal position.

TRPC1α generates strong pore field strength when assembles with TRPC4

The results above suggest that TRPC1α contributes to form a distinct pore when it heteromerizes with TRPC4. Next, we examined whether heteromerization with TRPC1α affects the permeability of TRPC4 and the preference for ions. Therefore, we prepared Na^+-rich ($[Na^+]_o$=140 mM), Li^+-rich ($[Li^+]_o$=140 mM), and Cs^+-rich ($[Cs^+]_o$=140 mM) solution and tested the relative monovalent cation permeability (P_X/P_{Na}) of M_3R-activated TRPC1α/4 channels.

Our results showed that the permeability for Na^+ ions was the highest in TRPC1α/4 channel and that for Cs^+

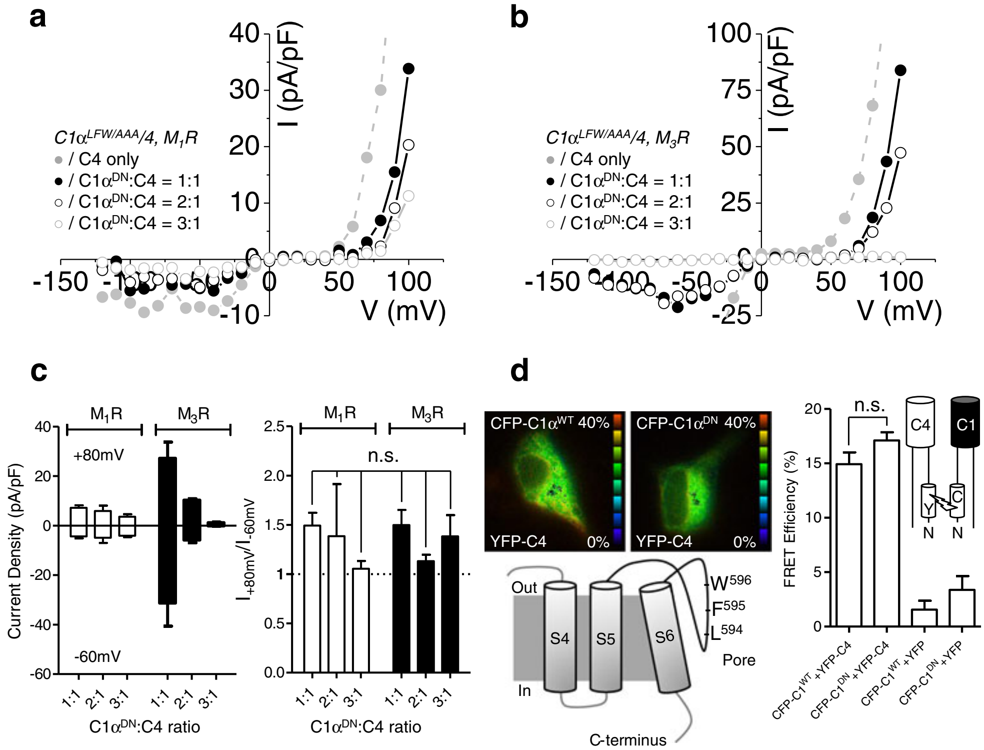

Fig. 2 Pore-constituting nature of TRPC1α in heteromeric formation with TRPC4 channel. **a** Effect of pore-dead TRPC1α (TRPC1α$^{LFW/AAA}$) on M_1R-activated TRPC1α/4 current. Expression of TRPC1α$^{LFW/AAA}$ abolished outward-rectifying *I–V* curves but only elicited small double-rectifying *I–V* curves. Increasing the dose of TRPC1α$^{LFW/AAA}$ cDNA up to three times to those of TRPC4 enhanced current suppression but maintained *I–V* signature to be double-rectifying shape. *Filled gray symbol* represents currents from cells expressing only TRPC4 channels; *filled black symbol* represents TRPC1α$^{LFW/AAA}$ cDNA:TRPC4 cDNA ratio of 1:1; *open black symbol* represents cDNA ratio of 2:1; *open gray symbol* represents cDNA ratio of 3:1. **b**Effect of pore-dead TRPC1α (TRPC1α$^{LFW/AAA}$) on M_3R-activated TRPC1α/4 current. The result was similar to M_1R-activated TRPC1α/4. Symbol notation is same to **a**. **c** *Left panel* represents summarized current densities measured above. Increasing the dose of TRPC1α$^{LFW/AAA}$ cDNA gradually suppressed current densities. *Right panel* represents current ratio between $I_{+80\text{mV}}$ and $I_{-60\text{ mV}}$. For all groups, rectification factors were not significantly different. **d** FRET measurement between CFP (donor) and YFP (acceptor) that were tagged to N-terminus of TRPC1α and TRPC4, respectively. Both of CFP-TRPC1α^{WT} and CFP-TRPC1α^{DN} showed significant FRET efficiency with YFP-TRPC4 while showing low FRET efficiency with YFP protein alone. *Inset diagram* depicts last three transmembrane domains (S4, S5, and S6) of TRPC1α and putative pore-forming domain spanning intermediate region between S5 and S6. L, F, W amino acids are located at positions 594, 595, and 596, respectively

ions was the lowest. Li^+ ions showed intermediate permeability (P_{Li}/P_{Na}=0.87±0.005, n=6; P_{Cs}/P_{Na}=0.77±0.005, n=6, Fig. 3a–c). This sequence of relative monovalent cation permeability ($P_{Na}>P_{Li}>P_{Cs}$) can be assigned to one of the Eisenmann sequences VIII, IX, and X [11], which are candidates of strong field pores. TRPC4 channels are known

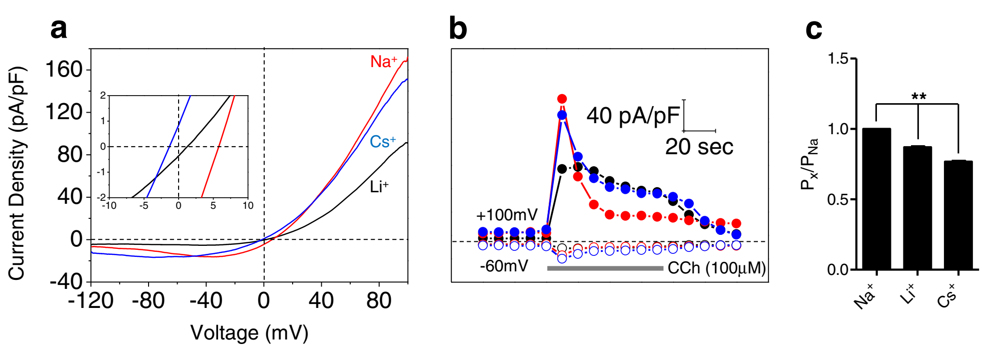

Fig. 3 Strong pore field strength of TRPC4 induced by heteromerization with TRPC1α. **a** Representative *I–V* curves of three monovalent cations—Li^+, Na^+, and Cs^+ ions. All three cations yielded typical outward-rectifying *I–V* curves. *Inset diagram* shows different reversal potentials. **b** Representative current traces of three monovalent cations. **c** Relative monovalent cation permeability (P_X/P_{Na}) among three monovalent cations. TRPC1α/4 showed highest monovalent cation permeability to Na^+ and lowest permeability to Cs^+

to have high Cs^+ to Na^+ permeability ratio (P_{Cs}/P_{Na}). They are also similarly permeable to Rb^+ ions and thereby are presumed to have weak pore strength.

Based on the generation of strong pore field strength and Eisenmann sequence, we suggest that TRPC1α not only contributes to form a distinct pore but also dramatically changes relative monovalent ion permeability of TRPC4.

Homomeric TRPC1β channel is not functional and TRPC1β/4 is less responsive to M_1 or M_3 stimulation than TRPC1α/4

In mammalian cells, TRPC1 is known to exist in two isoforms, i.e., unspliced TRPC1 (TRPC1α) and alternatively spliced TRPC1 (TRPC1β) [38, 44]. Figure 4a showed amino acid sequences of two isoforms (Fig. 4a). TRPC1β was prepared from TRPC1α via deletion mutation (see "Materials and methods") and cDNA of which was expressed in HEK293 cells with M1 and M3 receptors, respectively. Similar to TRPC1α, current response to M1 or M3 receptor stimulation was indistinguishable in cells expressing TRPC1β from cells expressing M1 or M3 receptor only (Fig. 4b, c). When TRPC4 was co-expressed with TRPC1β, however, CCh elicited currents with outwardly rectifying *I–V* relationship. Although CCh induced TRPC1β currents in all the cells tested (n=26), the current density was smaller than TRPC1α/4 channels. M_3R-activated current densities were 24.2±2.6and −3.0±0.5 pA/pF for TRPC1β/4 compared to 47.4±6.2 and −6.8±1.4 pA/pF for TRPC1α/4 (Fig. 4d–f, left and middle panel). Moreover, rectification factor ρ of TRPC1β/4 (11.3±1.5) was smaller than that of TRPC1α/4 channels (19.3±3.2) and thereby TRPC1β/4 is less efficient outward rectifier (Fig. 4f, right panel). FRET efficiency between CFP-tagged TRPC1β and YFP-tagged TRPC4 was 12.3±1.0 % which is significantly larger than the efficiency between YFP alone (3.3±1.1 %, Fig. 4g).

These results suggest that homomeric TRPC1β is not activated by muscarinic stimulation and TRPC1β/4 is less efficient outward rectifier than TRPC1α/4 channels.

$G\alpha_{i2}$ protein and $G_{i/o}$-coupled receptor stimulation selectively activates TRPC4 homomeric channels

Classical signal transduction pathway that has been suggested to activate TRPC channels was $G_{q/11}$-PLC pathway. Some focused on the hydrolysis of PIP_2, others on the generation of IP_3 and DAG, others on subsequent Ca^{2+} release or store-depletion [36]. Our group reported that $G\alpha_{i2}$ proteins and $G\alpha_{i3}$ proteins are novel and potent activators of TRPC4 and TRPC5 channels, respectively [15]. Since TRPC1 channel shares high amino acid sequence similarity with those two channels, we investigated whether $G\alpha_{i2}$ protein or $G_{i/o}$-coupled receptor stimulation is sufficient to activate TRPC1α channels. Instead of M1 or M3 receptor, M2 receptor (M_2R) or $G\alpha_{i2}{}^{Q205L}$ (intrinsic GTPase activity-deficient form of $G\alpha_{i2}$) was co-expressed with corresponding TRPC channels.

As shown previously [15], genuine TRPC4 homomeric channels showed characteristic double-rectifying *I–V* curves in response to M_2R stimulation by CCh or in $G\alpha_{i2}$-Cs^+-rich solution ($[Cs^+]_o$=140 mM) (Fig. 5a, b). TRPC1α channels, however, were not activated by such stimulations (Fig. 5c, d). TRPC1β showed similar results (Fig. 5g, h). Interestingly, CCh-stimulated whole-cell currents showed double rectifying *I–V* relationship when TRPC1α, TRPC4, and M_2R were co-expressed (n=17, Fig. 5e).

In TRPC1α/4+$G\alpha_{i2}{}^{Q205L}$ expressing cells, double-rectifying currents were measured (Fig. 5f). Similar investigation was conducted for cells expressing TRPC1β and TRPC4 channels. M_2R stimulation and $G\alpha_{i2}{}^{Q205L}$ protein all elicited double-rectifying *I–V* curves with significant response in current traces (Fig. 5i, j).

So far, M_2R stimulation and overexpression of $G\alpha_{i2}$ protein both yielded double-rectifying *I–V* curves which would be most likely come from homomeric TRPC4 channels. In such cases, the double-rectifying currents might have been predominant because only few TRPC1α/4 heteromers were expressed. Since the relative populations of TRPC1α, TRPC1α/4, and TRPC4 channels in plasma membrane are not definite, this time we facilitated the heteromeric assembly—TRPC1α/4—by increasing the relative dose of TRPC1α cDNA in heterologous transfection protocol. In other words, we facilitated the expression of TRPC1α in order that TRPC1α/4 heteromers would be assembled more dominantly than TRPC4 homomers. This would eventually increase the expected channel expression of TRPC1α/4 in sum. The result, however, showed constant double-rectifying *I–V* curves. This TRPC4-like current was remained up to TRPC1α/TRPC4 cDNA ratio of 1:1 but completely abolished when the ratio exceeds 2:1 (Fig. 6a–c). Incidence of TRPC1/4-like outward rectifying current was not increased as initially expected.

Lastly, we used combinatory pair of two different G-protein coupled receptors with different agonist specificity in order to confirm if M_2R stimulation selectively activates TRPC4 channels from plasma membrane where population of TRPC4 and TRPC1/4 channels are explicitly verified. One component of the receptor pair, M_2R, was used for $G_{i/o}$-TRPC4 activation while the other, H_1R (histamine receptor type 1), was used for $G_{q/11}$-TRPC1/4 activation. First, CCh (100 μM) was applied to stimulate M_2R and thereby turn on $G_{i/o}$ signaling. This would activate TRPC4 channels. After brief washout (less than 2 min), histamine (His, 10 μM) was applied to stimulate H_1R. This would turn on $G_{q/11}$ signaling and eventually activate TRPC1/4 channels. It is also possible that histamine activates not only TRPC1/4 channels but also TRPC4 channels. This is prevented, however, by pretreated carbachol; CCh-activated TRPC4 would be undergoing desensitization and would not respond to any of further activating stimulus.

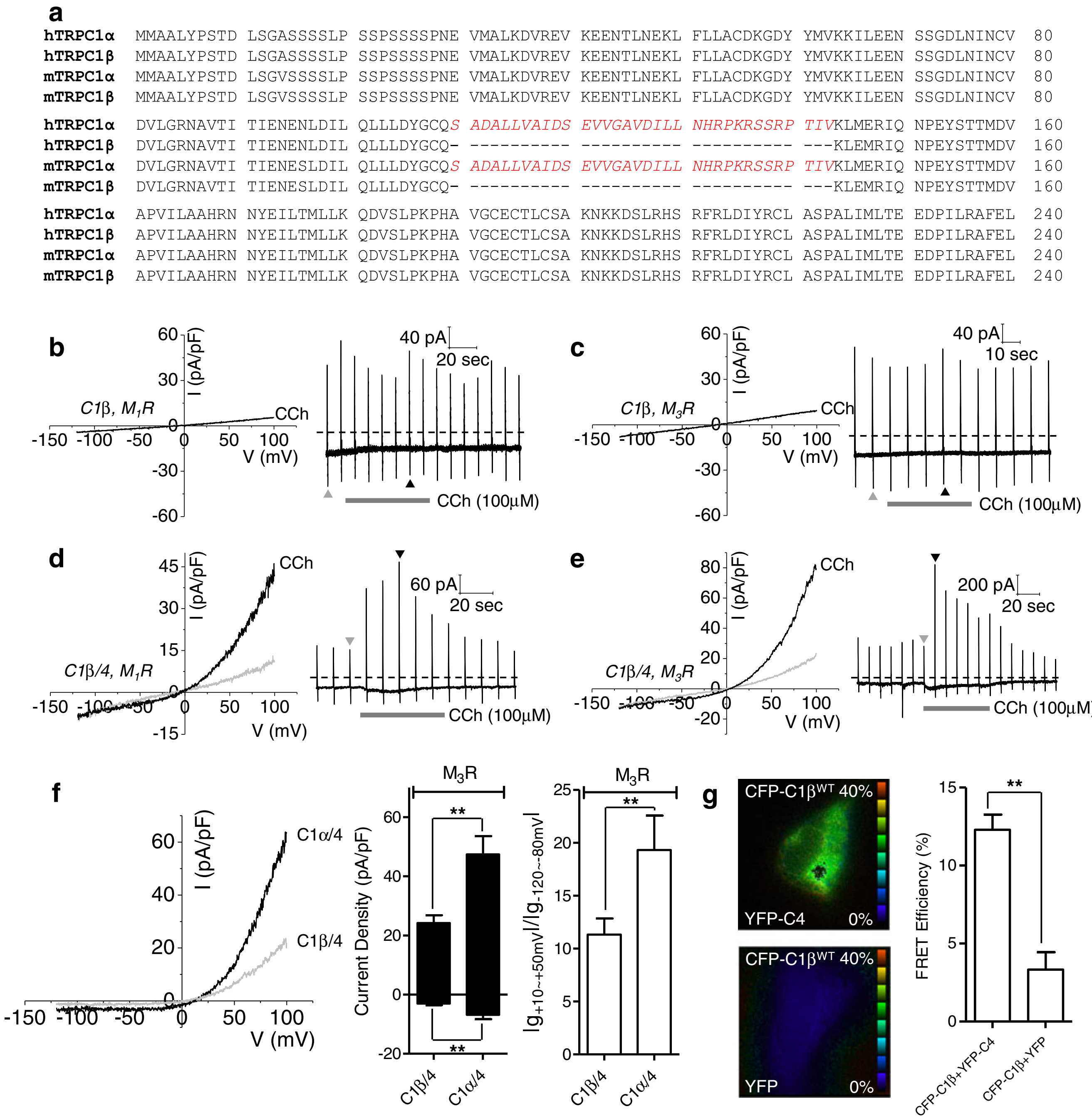

Fig. 4 TRPC1β and TRPC1β/4 channel activity in M1, M3 receptor stimulation system. **a** Amino acid sequences of human TRPC1 isoform long (hTRPC1α), isoform short (hTRPC1β), mouse TRPC1 isoform long (mTRPC1), and isoform short (mTRPC1β). Thirty-four amino acids from position 110 to 142 are missing in isoform short variants. **b**, **c** *I–V* relationship and current traces of cells expressing hTRPC1β and M1, M3 receptors, respectively. Extracellular carbachol (*CCh*, 100 μM) was insufficient to induce significant current increase for both groups. **d**, **e** *I–V* relationship and current traces of cells expressing hTRPC1β and TRPC4. M1 or M3 receptors were co-expressed, respectively. TRPC1β/4 channel was activated by muscarinic stimulation hence yielded outward-rectifying *I–V* relationship. **f** *Left panel* compares *I–V* curves of M_3R-activated TRPC1α/4 and TRPC1β/4 channels. Although TRPC1β/4 yields outward-rectifying *I–V* curves, current density and order of outward rectification were smaller than TRPC1α/4. *Middle panel* summarizes current densities and *right panel* indicates rectification factor *ρ*. **g** FRET measurement between CFP (donor) and YFP (acceptor) that were tagged to N-terminus of TRPC1β and TRPC4, respectively. CFP-TRPC1β showed significant FRET efficiency with YFP-TRPC4 while showing low FRET efficiency with YFP protein alone

As a result, H_1R stimulation successfully activated TRPC4 channels (Fig. 7a). TRPC1/4 channels were also activated by histamine (Fig. 7b). Co-expressed with M_2R and H_1R, TRPC4 permitted only a minute additional activation to histamine (4.08±1.53 %) once it was stimulated by carbachol (Supplementary Fig. 4). In cells expressing TRPC1, TRPC4,

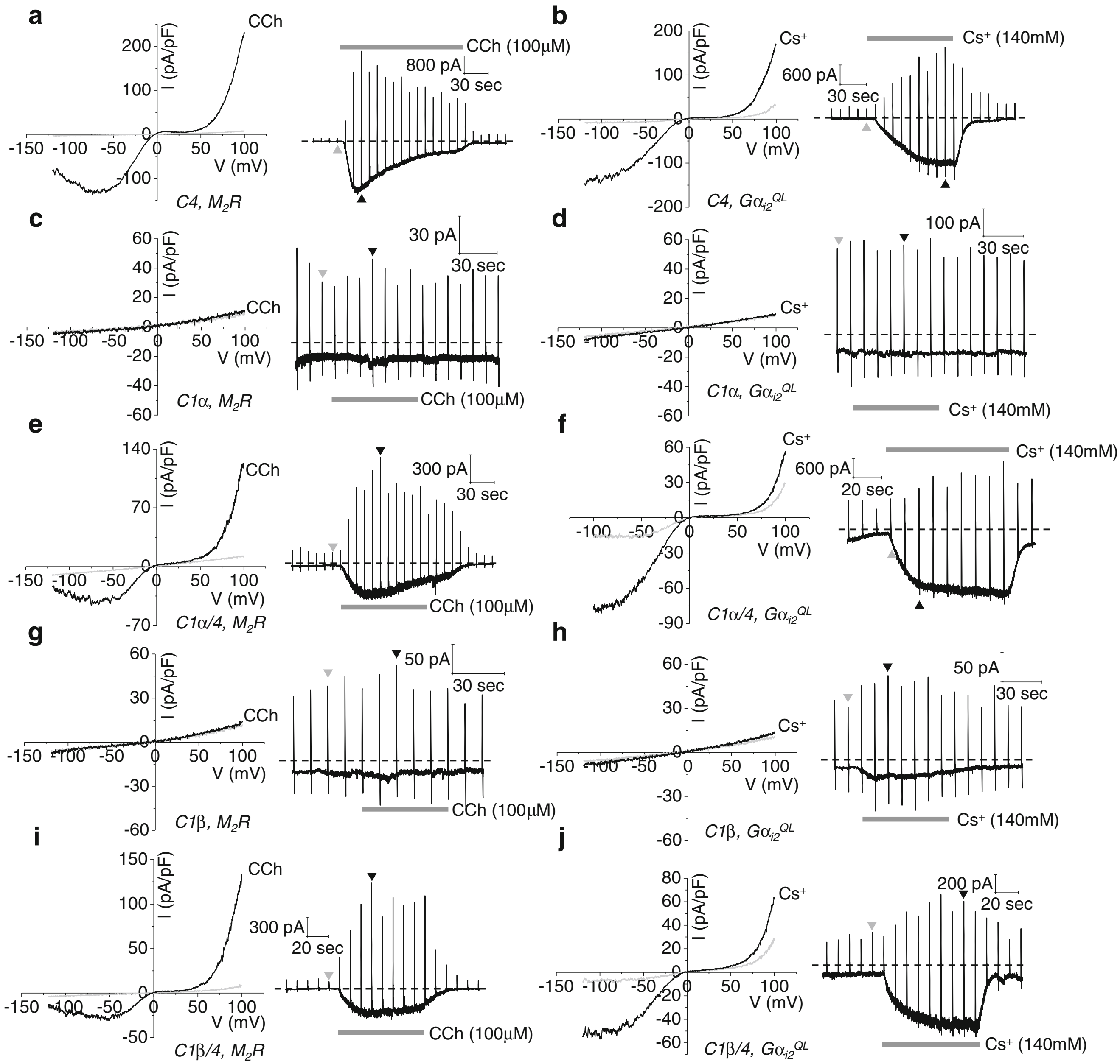

Fig. 5 TRPC1α, TRPC1α/4, and TRPC4 channel activities in response to $G_{i/o}$-coupled receptor (M2) stimulation and overexpression of $G\alpha_{i2}^{Q205L}$ protein. **a**, **b** Genuine TRPC4 homomeric channel activity in response to M2 receptor stimulation and overexpression of $G\alpha_{i2}^{Q205L}$ (intrinsic GTPase activity deficient mutant) protein. Extracellular carbachol (*CCh*, 100 μM) and Cs^+-rich solution ($[Cs^+]_o$=140 mM) was treated for each activation systems, respectively. TRPC4 channels activated by each condition showed typical double-rectifying *I–V* curves. **c**, **d** TRPC1α homomeric channel activities in response to M2 receptor and $G\alpha_{i2}^{Q205L}$ protein. Neither M2 receptor stimulation nor $G\alpha_{i2}^{Q205L}$ protein activated TRPC1α channels. **e**, **f** TRPC1α/4 heteromeric channel activities in response to M2 receptor and $G\alpha_{i2}^{Q205L}$ protein. Each activation system was insufficient to induce TRPC1α/4 channel currents but selectively activated TRPC4 homomeric channels. **g**, **h** TRPC1β homomeric channel activities in response to M2 receptor and $G\alpha_{i2}^{Q205L}$ protein. Both systems could not induce channel activation. **i**, **j** TRPC1β/4 heteromeric channel activities in response to M2 receptor and $G\alpha_{i2}^{Q205L}$ protein. Like TRPC1α/4, TRPC1β/4 did not permit their activation to those stimulators but only TRPC4 did permit their activation

H_1R, and M_2R, carbachol activated TRPC4 channels. In the same cell, subsequent histamine activated TRPC1/4 channels (Fig. 7c). The serial application of carbachol and histamine allowed us to measure functional populations of TRPC4 and TRPC1/4 channels. It was evident that histamine-activated TRPC1/4 population is small when carbachol-activated TRPC4 population is large and vice versa. In turn, negative correlation (Pearson's r=−0.94) between carbachol-activated TRPC4-like currents and histamine-activated TRPC1/4-like currents were obtainable (Fig. 7d). This result suggests that $G_{i/}$

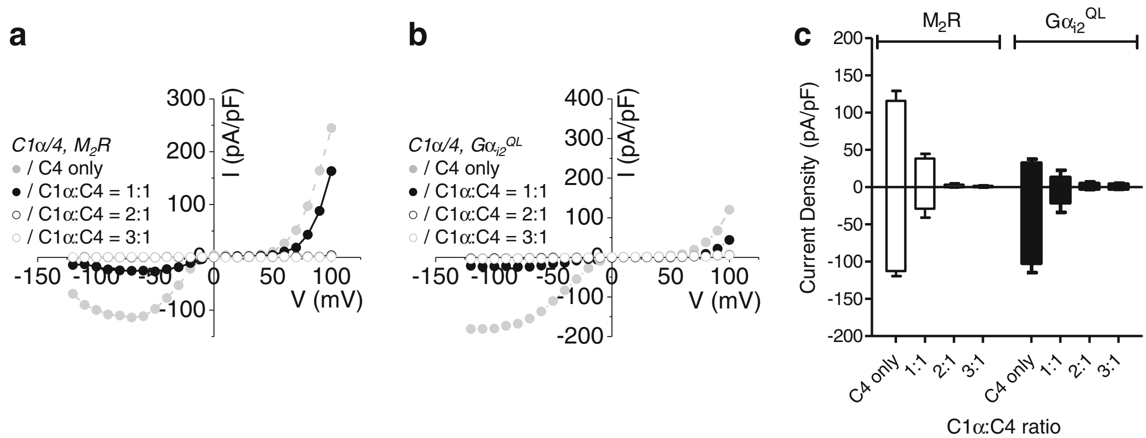

Fig. 6 Whole-cell current of M_2R-activated and $G\alpha_{i2}^{Q205L}$-activated TRPC4 from cells expressing massive TRPC1α and little TRPC4. **a** Under M_2R governance, increasing the dose of TRPC1α cDNA up to three times to those of TRPC4 could not induce any of M1R- or M3R-activated TRPC1α/4 current—outward-rectifying *I–V* curves. However, it enhanced current suppression while maintaining *I–V* signature to be double-rectifying shape. *Filled gray symbol* represents currents from cells expressing only TRPC4 channels; *filled black symbol* represents TRPC1α cDNA:TRPC4 cDNA ratio of 1:1; *open black symbol* represents cDNA ratio of 2:1; *open gray symbol* represents cDNA ratio of 3:1. **b** Under $G\alpha_{i2}^{Q205L}$ activation system, increasing the dose of TRPC1α cDNA up to three times to those of TRPC4 could not induce any of M1R- or M3R-activated TRPC1α/4 current—outward-rectifying *I–V* curves. Results were similar to M_2R-activated groups. **c** Summarized whole-cell current density of cells expressing various levels of TRPC1α and TRPC4 cDNAs. Double-rectifying *I–V* curves were completely abolished as relative cDNA amount of TRPC1α to TRPC4 exceeds 2

$_o$-coupled receptor discriminates TRPC4 channels from plasma membrane pool where TRPC4 and TRPC1/4 channels coexist and selectively activates the former.

Taken together, we conclude that M_2R stimulation and $G\alpha_{i2}$ protein selectively activates TRPC4 channels regardless of relative populations of TRPC1α/4 and TRPC4 channels.

Discussion

Highly sensitive electrophysiological recordings revealed that whole cell currents from cells expressing TRPC1α and TRPC1β were not different from cells expressing only M1 or M3 receptors. Rigorously speaking, it seems that both of TRPC1α and TRPC1β are not able to form a functional ion channel in plasma membrane alone based on their surface levels. These results demonstrate that TRPC1 isoforms (long TRPC1α and short TRPC1β) do not respond to muscarinic stimulation, possibly due to the facts that these homomeric channels were unable to homotetramerize or inserted into plasma membrane [13].

Heteromerized with TRPC4, however, TRPC1 was successfully located into plasma membrane as equal constituents and it altered the properties of TRPC4 (from double rectifying) to outwardly rectifying TRPC1/4. Heteromerization has been shown previously [29], but in this study, we performed functional assay by using pore-dead mutation and whole-cell recording. Pore-dead mutant of TRPC1α successfully assembled with TRPC4 and suppressed the M1- or M3-activated TRPC1α/4 channel current. The result ruled out the possibility of TRPC1α being β ancillary subunit. Responsible for quartet assembly, TRPC1α, an α subunit, not only contributes to form a novel pore but changes relative monovalent cation permeability of TRPC4 channels and pore strength.

The isoform specificity of TRPC1 channel in heteromeric formation with TRPC4 was striking. TRPC1α/4 was far more sensitive than TRPC1β/4 to $G_{q/11}$-coupled receptor stimulation. TRPC1β lacks 34 amino acids from position 110 to 143. Located in the N-terminus, this region spans two or three amino acids of last ankyrin-like repeat domain 2 (ANK2) and intermediate region that links ANK2 and ANK3 domains. Therefore, alternative splicing in this region may be obligatory to isoform-specific channel property of TRPC1α/4 and TRPC1β/4 channels.

Lastly, whereas TRPC1/4 channels are activated by $G_{q/11}$-coupled receptor stimulation, they are not sensitive to $G_{i/o}$-coupled receptors. $G_{i/o}$-coupled receptor selectively activates TRPC4 homomeric channels. Similarly, $G\alpha_{i2}^{Q205L}$ proteins activated TRPC4 homomeric channels but not TRPC1/4 heteromeric channels. If the activation of TRPC4 subunit (two monomers) in TRPC1/4 channels is sufficient for activation of tetramer, then TRPC1/4 could have opened by M_2R stimulation by carbachol. One possible explanation for this premise is that TRPC1 somewhat hinders the binding of $G\alpha_{i2}$ protein onto TRPC4 subunit. In a sense, it is interesting that TRPC1 lacks one of TRPC4-$G\alpha_{i2}$ binding interface: RNLVKR amino acids. When aligned with TRPC4 and TRPC5, TRPC1 does not have lysine at similar position (K^{715} for mTRPC4β). Both of TRPC4 and TRPC5 have RN residue but is changed to two cysteines in TRPC1 (Supplementary Fig. 5).

The other premise is that TRPC1 changes the gating mechanism *per se* and does not allow $G\alpha_i$ protein to sufficiently

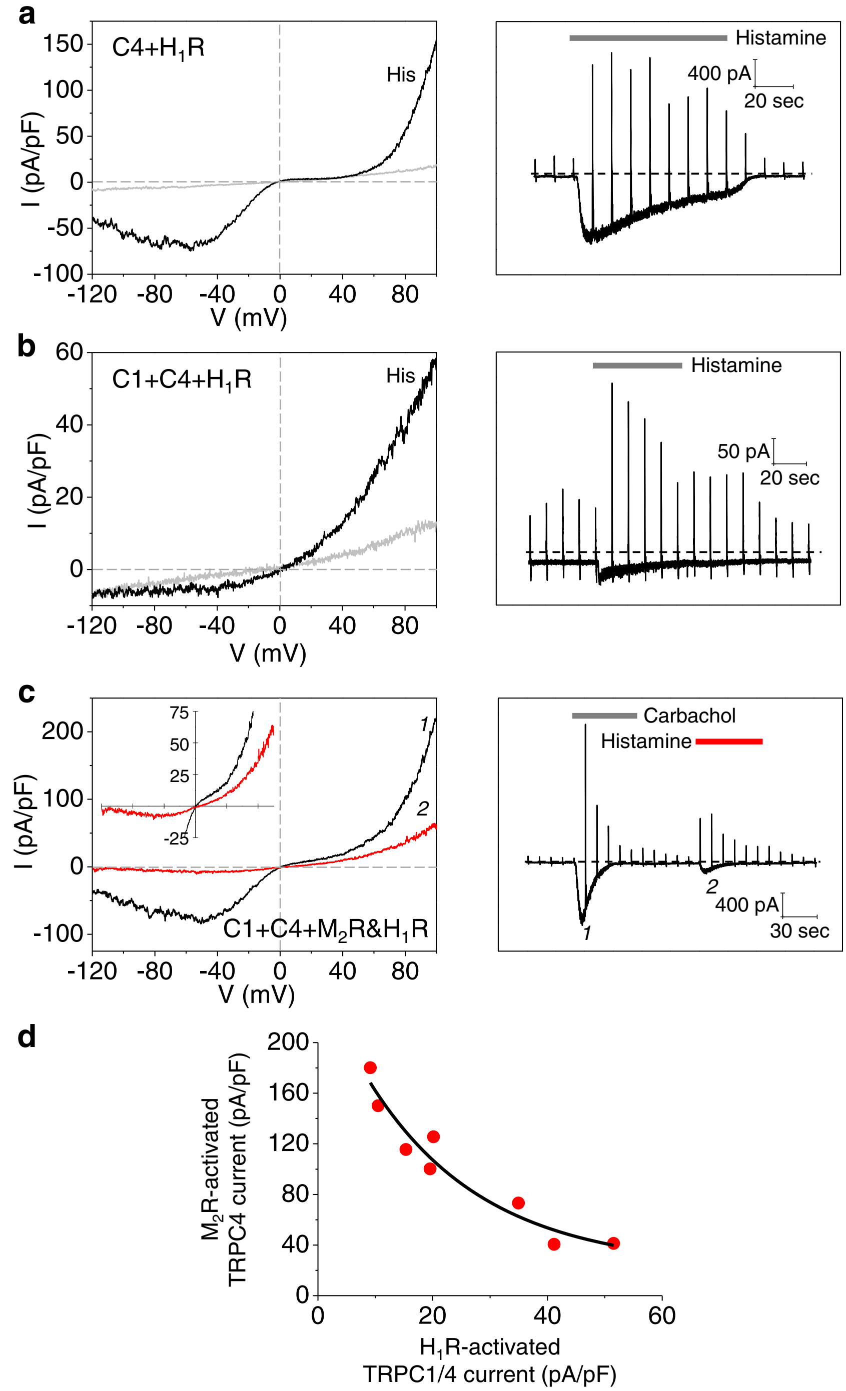

Fig. 7 Selective activation of M2 receptor onto TRPC4. **a** Histamine receptor type 1 (*H_1R*), a $G_{q/11}$-coupled receptor, activates TRPC4 channel as M1 or M3 receptor does. *Black line* indicates current after histamine was introduced and *light gray line* indicates basal current. **b** TRPC1/4-like outwardly-rectifying currents were obtained when histamine receptor was stimulated by extracellular histamine (*His*, 10 μM). **c** Serial application of carbachol and histamine activated TRPC4 channel and TRPC1/4 channel, respectively and sequentially. M2 receptor selectively activated TRPC4 channels where expression of TRPC1/4 in a given cell is confirmed by H1 receptor stimulation. *Black line* indicates carbachol-M_2R-activated current and *red line* indicates histamine-H_1R-activated current. **d** Negative correlation between current amplitude of M_2R-activated TRPC4 and H_1R-activated TRPC1/4 channels. Given that capacity for ion channels in plasma membrane is conservative, relative population between TRPC4 and TRPC1/4 channels must be in inverse relationship. *Red dots* represent each data points and *black line* is their fitting into exponential decay function. Pearson product–moment correlation coefficient (PPMCC, *r*) was −0.94

activate TRPC1/4 channels. This case TRPC1 would close one potent activation mechanism—$G\alpha_i$—but leave the other classical activation mechanism intact—$G\alpha_q$. Molecular gating mechanism of TRPC1/4 channel is still unknown and further investigation is necessary.

The prevalence of TRPC1 compared to TRPC4 or TRPC5 channel in various organs and tissues suggests that TRPC1 is a channel that plays important physiological roles in humans. TRPC1s are also expected to have diverse functionality to fulfill its multifaceted roles. Accumulating evidences over the years support that TRPC1 channels are mediators of SOCE [5, 7, 17, 26, 31, 32, 42, 45]. In general, thapsigargin- or CPA-mediated store depletion is sufficient to induce Ca^{2+} influx as well as inward Na^+ current. Although store-operated Ca^{2+} influx was primarily underpinned by Ca^{2+} measurement with patch-clamping being relatively shallow (even so, mostly in single-channel configuration rather than whole-cell recording [21]), the consensus made by these groups seemed to be without any disproof. In salivary gland, TRPC1 was shown to function as a SOCE mediator [17, 18]. Indeed, it is generally accepted that TRPC1 may operate as a SOCE mediator especially at non-excitable cells or tissues.

In vascular smooth muscle cells, however, two contrasting studies were reported [6, 30]. Using TRPC1$^{-/-}$ mouse model, one group suggests that the whole-cell current measurement in mesenteric artery following store depletion was mediated by TRPC1/5 channels. Using the same model, the other group showed that TRPC1 was not obligatory to cation influx in cerebral artery VSMCs. In essence, whether TRPC1 functions as a SOCE mediator in various tissues remains to be elucidated.

Similarly, the role of TRPC4 has also been controversial. It is suggested to be SOCE mediator or receptor-operated Ca^{2+} entry. TRPC5 is regulated and activated by even more various factors such as La^{3+}, Gd^{3+}, lysophosphatidylcholine, reducing and oxidizing agents (DTNP, DTT), isoprenaline, forskolin, and 8-Br-cAMP [3, 14]. Store depletion was also suggested to activate TRPC5 [16, 25, 43]. Hence, TRPC5 has been suggested to be “multifunctional” due to the various activation patterns [3].

Although our results show complex properties of TRPC1α, TRPC1β, TRPC1α/4, and TRPC1β/4, given that TRPC1 is multifunctional [2], would it not be possible that the complex results reflect distinct electrophysiology property of TRPC1—multifunction?

Although evidences of the physiological significance of TRPC1 channel and its characteristics are emerging, molecular or sub-molecular activation mechanism is still unknown. Our present work and that of others [33, 34] suggest that TRPC1/4 channel is undoubtedly a receptor-operated channel, whether it is mutually exclusive to store depletion or not. So far, $G_{q/11}$-PLC pathway has been considered as the primary candidate to activate TRPC1α/4. In the present study, we observed outward-rectifying *I–V* signature of TRPC1α/4 channel in all of M1, M2, and M3 receptor activation systems (M2 receptor stimulation yielded outward-rectifying signatures though probability was significantly lower (6 %, 3/20) than M1 or M3 stimulation (100 %, 6/6 (M1), 31/31 (M3)). In other words, although we believe that selective $G_{i/o}$-coupled receptor activation discriminates TRPC4 homomeric channels from ion channel pools on the plasma membrane, the common molecular candidate (e.g., $G_{\beta\gamma}$ subunits, $[Ca^{2+}]_i$ increase) that is/are shared among M1, M2, and M3 receptor might activate TRPC1α/4 channels (Fig. 8a). Thorough investigations are necessary to underpin the detailed mechanisms of TRPC1 activation.

In GI tract, M2 and M3 receptors coexist with TRPC1, TRPC 4, or TRPC 6 channels. Recent experiments with M2, M3 single or double knockout mice showed interesting results. M2$^{-/-}$ showed 120pS and 70pS single channel conductance with minor 20pS conductance whereas M3$^{-/-}$ showed only 70pS conductance with minor 20pS conductance [28]. In another study conducted in murine ileal myocytes [37], three cation conductances, 7pS, 55pS, and 116pS, were measured. Using RT-PCR, they also suggested that mRNA levels of TRPC4, TRPC6, and TRPC1 are high in murine ileal myocytes. Cation influx through the cation conductance was completely abolished when TRPC4 and TRPC6 were double-knocked out. Thus, 120pS (or 116pS) conductance was surmised to be TRPC6 conductance activated by M3 stimulation while 70pS (or 55pS) conductance to be TRPC4 activated by both M3 and/or M2 stimulation. Although single channel recording and rigorous analysis must be made prior to the postulation, we believe that minor 20pS (or 7pS) conductance is from TRPC1/4 channels. In addition, the typical U-shaped *I–V* curves obtained at endogenous GI tract is in contrast to outward-rectifying TRPC1/4 *I–V* curves. Having remarked similar mRNA levels of TRPC1, TRPC 4, and TRPC 6 channels in GI tract [37], we surmise that M2 governance in GI tract discriminate TRPC4 from TRPC1/4 and selectively activates it and yield U-shape *I–V* curves.

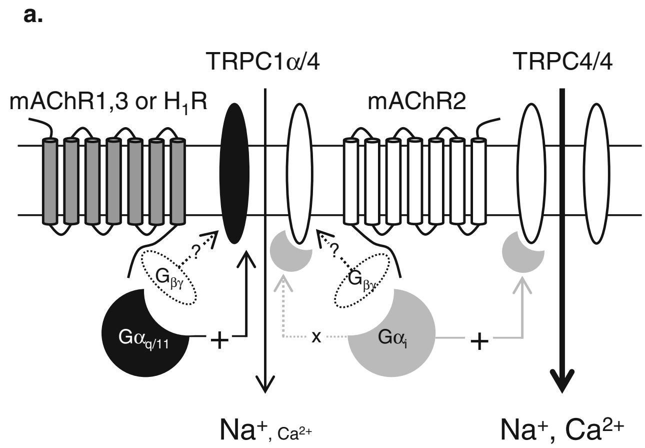

Fig. 8 Conclusive diagram concerning TRPC1α/4, TRPC4 channels and G-protein coupled receptors. **a** $G_{q/11}$-coupled receptor stimulation activates TRPC1α/4 channels but $G_{i/o}$-coupled receptor stimulation is insufficient to do so. However, the $G_{i/o}$-coupled receptor discriminates TRPC4 homomeric channels from TRPC1α/4 channels and selectively activates the former. The Ca^{2+} permeability difference between those two channels was reported by Storch et al. [33]. The roles of $G_{\beta\gamma}$ subunits shared among muscarinic receptors are so far unknown

Acknowledgements We thank Dr. Michael Mederos and Dr. Thomas Gudermann for kindly donating human TRPC1 isoform long (hTRPC1α) construct and Dr. Vaca Luis for kindly donating CFP-hTRPC1 isoform long and YFP-hTRPC1 isoform long constructs. We thank Dr. Young Duk Yang for kindly donating rat histamine receptor type 1. We thank Dr. Yin Hua Zhang for kindly revising the manuscript. We acknowledge the roles of the Biomedical Imaging Center at the Seoul National University College of Medicine, Seoul, Korea. This study was supported by grant from the National Research Foundation of Korea funded by the Korea government (MEST) (2012R1A2A1A01003073) and Seoul National University Hospital Research Fund (03-2012-0140) (I. So).

Conflict of interest The authors declare no conflict of interest.

References

1. Ambudkar IS (2006) Ca^{2+} signaling microdomains: platforms for the assembly and regulation of TRPC channels. Trends Pharmacol Sci 27:25–32
2. Beech DJ (2005) TRPC1: store-operated channel and more. Pflugers Arch Eur J Physiol 451:53–60
3. Beech DJ (2007) Canonical transient receptor potential 5. Handb Exp Pharmacol 179:109–123
4. Corpet F (1988) Multiple sequence alignment with hierarchical clustering. Nucleic Acids Res 16:10881–10890
5. Delmas P, Wanaverbecq N, Abogadie FC, Mistry M, Brown DA (2002) Signaling microdomains define the specificity of receptor-mediated IP_3 pathways in neurons. Neuron 34:209–220
6. Dietrich A, Kalwa H, Storch U, Schnitzler MM, Salanova B, Pinkenburg O, Dubrovska G et al (2007) Pressure-induced and store-operated cation influx in vascular smooth muscle cells is independent of TRPC1. Pflugers Arch Eur J Physiol 455:465–477
7. Engelke M, Friedrich O, Budde P, Schaefer C, Niemann U, Zitt C, Jungling E, Rocks O, Luckhoff A, Frey J (2002) Structural domains required for channel function of the mouse transient receptor potential protein homologue TRP1β. FEBS Lett 523:193–199
8. Erickson MG, Alseikhan BA, Peterson BZ, Yue DT (2001) Preassociation of calmodulin with voltage-gated Ca^{2+} channels revealed by FRET in single living cells. Neuron 31:973–985
9. Fruhwald J, Londono JC, Dembla S, Mannebach S, Lis A, Drews A, Wissenbach U, Oberwinkler J, Philipp SE (2012) Alternative splicing of a protein domain indispensable for function of transient receptor potential melastatin 3 (TRPM3) ion channels. J Biol Chem 287:36663–36672
10. Goldman DE (1943) Potential impedance and rectification in membranes. J Gen Physiol 27:37–60
11. Hille B (2001) Ion channels of excitable membranes, 3rd edn. Sinauer Associates, Sunderland
12. Hodgkin AL, Katz B (1949) The effect of sodium ions on the electrical activity of the giant axon of the squid. J Physiol 148:127–160
13. Hofmann T, Schaefer M, Schultz G, Gudermann T (2002) Subunit composition of mammalian transient receptor potential channels in living cells. Proc Natl Acad Sci 99:7461–7466
14. Hong C, Kim J, Jeon JP, Wie J, Kwak M, Ha K, Kim H, Myeong J, Kim SY, Jeon JH, So I (2012) Gs cascade regulates canonical transient receptor potential 5 (TRPC5) through cAMP mediated intracellular Ca^{2+} increase and ion channel trafficking. Biochem Biophys Res Comm 421:105–111
15. Jeon JP, Hong C, Park EJ, Jeon JH, Cho NH, Kim IG, Choe H, Muallem S, Kim HJ, So I (2012) Selective $G\alpha_i$ subunits as novel direct activators of transient receptor potential canonical (TRPC)4 and TRPC5 channels. J Biol Chem 287:17029–17039
16. Kanki H, Kinoshita M, Akaike A, Satoh M, Mori Y, Kaneko S (2001) Activation of inositol 1,4,5-triphosphate receptor is essential for the opening of mouse TRP5 channels. Mol Pharmacol 60:989–998
17. Liu X, Wang W, Singh BB, Lockwich T, Jadlowiec J, O' Connell B, Wellner R, Zhu MX, Ambudkar IS (2000) Trp1, a candidate protein for the store-operated Ca^{2+} influx mechanism in salivary gland cells. J Biol Chem 275:3403–3411
18. Liu X, Singh BB, Ambudkar IS (2003) TRPC1 is required for functional store-operated Ca^{2+} channels. J Biol Chem 278:11337–11343
19. Montell C (1997) New light on TRP and TRPL. Mol Pharmacol 52:755–763
20. Nilius B (2003) From TRPs to SOCs, CCEs, and CRACs: consensus and controversies. Cell Calcium 33:293–298
21. Nilius B (2004) Store-operated Ca^{2+} entry channels: still elusive! Sci STKE 243:pe36
22. Oberwinkler J, Lis A, Giehl KM, Flockerzi V, Philipp SE (2005) Alternative splicing switches the divalent cation selectivity of TRPM3 channels. J Biol Chem 280:22540–22548
23. Otsuguro K, Tang J, Tang Y, Xiao R, Freichel M, Tsvilovskyy V, Ito S, Flockerzi V, Zhu MX, Zholos AV (2008) Isoform-specific inhibition of TRPC4 channel by phosphatidylinositol 4,5-bisphosphate. J Biol Chem 283:10026–10036
24. Parekh A, Putney J (2005) Store-operated calcium channels. Physiol Rev 85:757–810
25. Philipp S, Hambrecht J, Braslavski L, Schroth G, Freichel M, Murakami M, Cavalie A, Flockerzi V (1998) A novel capacitative calcium entry channel expressed in excitable cells. EMBO J 17:4274–4282
26. Rao JN, Platoshyn O, Golovina VA, Liu L, Zou T, Marasa BS, et al., TRPC1 functions as a store-operated Ca^{2+} channel in intestinal epithelial cells and regulates early mucosal restitution after wounding. Am J Physiol Gastrointest Liver Physiol 290:G782-G792
27. Rychkov G, Barritt GJ (2007) TRPC1 Ca^{2+}-permeable channels in animal cells. Handb Exp Pharmacol 179:23–52
28. Sakamoto T, Unno T, Kitazawa T, Taneike T, Yamada M, Wess J, Nishimura M, Komori S (2007) Three distinct muscarinic signaling pathways for cationic channel activation in mouse gut smooth muscle cells. J Physiol 582:41–61
29. Schaefer M (2005) Homo- and heteromeric assembly of TRP channel subunits. Pflugers Arch Eur J Physiol 451:35–42
30. Shi J, Ju M, Abramowitz J, Large WA, Birnbaumer L, Albert AP (2012) TRPC1 proteins confer PKC and phosphoinositol activation on native heteromeric TRPC1/C5 channels in vascular smooth muscle: comparative study of wild-type and TRPC1−/− mice. FASEB 26:409–419
31. Sinkins WG, Estacion M, Schilling WP (1998) Functional expression of TRPC1: a human homologue of the *Drosophila* TRP channel. Biochem J 331:331–339
32. Sours S, Du J, Chu S, Ding M, Zhou XJ, Ma R (2006) Expression of canonical transient receptor potential (TRPC) proteins in human glomerular mesangial cells. Am J Physiol Renal Physiol 290:F1507–F1515
33. Storch U, Forst AL, Philipp M, Gudermann T, Schnitzler MM (2012) Transient receptor potential channel 1 (TRPC1) reduces calcium permeability in heteromeric channel complexes. J Biol Chem 287:3530–3540
34. Strubing C, Krapivinsky G, Krapivinsky L, Clapham DE (2001) TRPC1 and TRPC5 form a novel cation channel in mammalian brain. Neuron 29:645–655
35. Strubing C, Krapivinsky G, Krapivinsky L, Clapham DE (2003) Formation of novel TRPC channels by complex subunit interactions in embryonic brain. J Biol Chem 278:39014–39019
36. Sukumar P, Sedo A, Li J, Wilson LA, O' Regan D, Lippiat JD, Porter KE, Kearney MT, Ainscough JFX, Beech DJ (2012) Constitutively active TRPC channels of adipocytes confer a mechanism for sensing dietary fatty acids and regulating adiponectin. Circ Res 111:191–200
37. Tsvilovskyy VV, Zholos AV, Aberle T, Philipp SE, Dietrich A, Zhu MX, Birnbaumer L, Freichel M, Flockerzi V (2009) Deletion of TRPC4 and TRPC6 in mice impairs smooth muscle contraction and intestinal motility *in vivo*. Gastroenterology 137:1415–1424
38. Vasquez E, Valverde MA (2006) A review of TRP channels splicing. Semin Cell Dev Biol 17:607–617
39. Venkatachalam K, Montell C (2007) TRP channels. Annu Rev Biochem 76:387–417
40. Villereal ML (2006) Mechanism and functional significance of TRPC channel multimerization. Semin Cell Dev Biol 17:618–629
41. Wes PD, Chevesich J, Jeromin A, Rosenberg C, Stetten G, Montell C (1995) TRPC1, a human homolog of a *Drosophila* store-operated channel. Proc Natl Acad Sci 92:9652–9656

42. Yuan JP, Kiselyov K, Shin DM, Chen J, Shcheynikov N, Kang SH, Dehoff MH, Schwarz MK, Seeburg PH, Muallem S, Worley PF (2003) Homer binds TRPC family channels and is required for gating of TRPC1 by IP_3 receptors. Cell 114:777–789
43. Zeng F, Xu SZ, Jackson PK, McHugh D, Kumar B, Fountain SJ, Beech DJ (2004) Human TRPC5 channel activated by a multiplicity of signals in a single cell. J Physiol 559:739–750
44. Zhu X, Chu PB, Peyton M, Birnbaumer L (1995) Molecular cloning of a widely expressed human homologue for the *Drosophila trp* gene. FEBS Lett 373:193–198
45. Zitt C, Zobel A, Obukhov AG, Harteneck C, Kalkbrenner F, Luckhoff A, Schultz G (1996) Cloning and functional expression of a human Ca^{2+}-permeable cation channel activated by calcium store depletion. Neuron 16:1189–1196